

Article

Sodium Silicates Modified Calcium Oxide as a High-Performance Solid Base Catalyst for Biodiesel Production

Shunpan Zhang^{1,2,3,4}, Junying Fu^{1,2,3,*}, Shiyou Xing^{1,2,3}, Ming Li^{1,2,3}, Xiaochun Liu^{1,2,3,5} , Lingmei Yang^{1,2,3} and Pengmei Lv^{1,2,3,*}

¹ Guangzhou Institute of Energy Conversion, Chinese Academy of Sciences, Guangzhou 510640, China; zhangshunpan20@mails.ucas.ac.cn (S.Z.); xingsy@ms.giec.ac.cn (S.X.); liming@ms.giec.ac.cn (M.L.); liuxiaochun@mail.ustc.edu.cn (X.L.); yanglm@ms.giec.ac.cn (L.Y.)

² CAS Key Laboratory of Renewable Energy, Guangzhou 510640, China

³ Guangdong Provincial Key Laboratory of New and Renewable Energy Research and Development, Guangzhou 510640, China

⁴ University of Chinese Academy of Sciences, Beijing 100049, China

⁵ School of Energy Science and Engineering, University of Science and Technology of China, Hefei 230026, China

* Correspondence: fujy@ms.giec.ac.cn (J.F.); lvpm@ms.giec.ac.cn (P.L.)

Abstract: Under the energy crisis and with greenhouse gases causing an ecological imbalance, biofuel has attracted worldwide attention due to its sustainability and low net-carbon emission. For years, the traditional biodiesel industry has been demanding a high-performance solid base catalyst. Its poor reusability is the bottleneck for a promising calcium-based solid-base catalyst. In this work, we successfully adopted a new silicate-strength strategy to improve the stability while preserving the activity of the catalyst. The newly synthesized catalyst, NCSO, had two main catalytic phases, Na₂CaSiO₄ and CaO, and showed a 98.2% FAMEs yield in 60 min at 80 °C with a methanol/oil molar ratio of 9:1 and 5 wt.% catalyst loading. After 12 consecutive reuses, a 57.3% FAMEs yield could still be achieved. The effect of the reaction temperature, methanol ratio, catalyst loading, and reaction time on the FAMEs yield was also investigated. With a combined characterization of XRD, XPS, and SEM, etc., we confirmed that Na₂CaSiO₄ and CaO showed a synergistic effect in catalyzing the transesterification reaction: the addition of the Na₂CaSiO₄ phase in NCSO could significantly improve the activity of CaO, while the CaO phase, in turn, helps to stabilize the Na₂CaSiO₄ phase. This silicate-strength strategy provides a new route to synthesize stable and highly active solid base catalysts.

Keywords: biodiesel; transesterification; solid base catalyst; silicate-strength strategy



Citation: Zhang, S.; Fu, J.; Xing, S.; Li, M.; Liu, X.; Yang, L.; Lv, P. Sodium Silicates Modified Calcium Oxide as a High-Performance Solid Base Catalyst for Biodiesel Production. *Catalysts* **2023**, *13*, 775. <https://doi.org/10.3390/catal13040775>

Academic Editors: Domenico Licursi and Juan Hernández Adrover

Received: 10 March 2023

Revised: 6 April 2023

Accepted: 14 April 2023

Published: 20 April 2023



Copyright: © 2023 by the authors. Licensee MDPI, Basel, Switzerland. This article is an open access article distributed under the terms and conditions of the Creative Commons Attribution (CC BY) license (<https://creativecommons.org/licenses/by/4.0/>).

1. Introduction

With the development of the world economy, energy demand is increasing daily. However, the limited reserve of traditional fossil fuels is causing energy insecurity, and the extra emission of CO₂ is challenging the global ecological environment [1–3]. The development of new, environmentally friendly, non-fossil fuels is quite urgent [4]. Biodiesel has attracted worldwide attention due to its lower sulfuric content/toxicity, better lubricity than petroleum diesel, and compatibility with traditional engines [5–7]. It can effectively replace or mix with fossil fuels, thereby reducing greenhouse gas emissions, benefitting the environment and alleviating the energy crisis. Generally, biodiesel can be synthesized by the transesterification of animal and vegetable oils, waste oils, microalgae, and microbial oils with short-chain alcohols (mainly methanol) [8]. The catalyst is the key component of this reaction, and traditionally, homogeneous base catalysts such as KOH and NaOH are often used in the transesterification reaction under mild reaction conditions. However, these catalysts cannot be recycled, thus reducing the biodiesel quality and causing unnecessary

water waste (to remove residue catalyst in biodiesel), making by-product glycerol hard to refine [9]. Due to their recyclability advantages, heterogeneous solid base catalysts have received extensive attention from researchers. A lot of research has been conducted with CaO (calcium oxide), a potential solid base catalyst with relatively high activity, low cost, low solubility in methanol, low toxicity, and recyclability [10–13], to find a way to up-scale its application in the biodiesel industry. Some researchers have used base or other metal elements to dope CaO to improve its transesterification activity [14]. Teo et al. [15] synthesized CaO-MgO catalysts by the co-precipitation method and found that the mixed solid base oxides (Ca/Mg = 1, molar ratio) exhibited a relatively higher basicity and stability among all of the researched samples. Rabie et al. [11] prepared a new type of basic heterogeneous catalyst with a CaO/MgO composite loaded on diatomite. They found that the diatomaceous earth support could significantly increase the total porosity and surface area of the catalyst, with a biodiesel yield as high as 96.47%. Kandis Sudsakorn et al. [16] synthesized strontium (Sr)-doped CaO/MgO catalysts and their results showed that the Sr²⁺ could provide many strong basic sites over CaO/MgO, and a FAME (fatty acid methyl ester) yield of 99.6% was obtained under the optimal conditions.

However, the bottleneck of CaO as a base catalyst is its deactivation by leaching during the reaction, thus shortening its working life [17]. To improve the reusability of solid base catalysts, supports such as nano-tubes, aluminate salts, and silicate salts have been investigated [18–24]. Mohd Lokman Ibrahim increased the basicity of the catalyst by loading sodium oxide onto carbon nanotubes. As a carrier, carbon nanotubes have super high compatibility with sodium oxide, and the best yield of FAME was 97.6% [22]. Behgam et al. [20] synthesized MgAl₂O₄ by the combustion method and then deposited MgO on the surface of the catalyst by the impregnation method. They found that MgO/MgAl₂O₄ showed a good reusability of six times and kept an 80% FAME yield. Wang et al. [25] found that the silicate phases, Ca₂MgSi₂O₇, in a gasified straw slag showed high reusability in catalyzing transesterification reactions. It could be reused for up to 50 cycles with over 50% of the maximum activity remaining. They also found that other bimetallic silicates also showed high reusability. However, these catalysts often required severe reaction conditions such as 160 °C or higher reaction temperatures, and 8 h or longer reaction times [26,27]. Liu et al. designed a Ca-based solid base catalyst modified by Na₂SiO₃ and the catalyst showed much better water and carbon dioxide resistance than CaO [8]. These results confirmed that the silicate modification could indeed improve the reusability of the Ca-based solid base catalyst, and the [SiO₄] tetrahedron structures in the researched silicates seemed to be the main reason for improving the stability of the catalyst. However, research is still needed to further improve the activity of the silicate-modified Ca-based solid base. Romero et al. [21] synthesized Na₂ZnSiO₄ as a catalyst by doping sodium into ZnSi-O, and the catalyst showed a biodiesel yield higher than 99% within 45 min. Stefan M. Pavlović et al. synthesized calcium silicate loaded with CaO, which showed a 97.8% FAME yield in 30 min [28]. Although these studies claimed that the silicate modification could also show good activity, these catalysts could only last for five reused times. Thus, a better silicate modification method is needed to improve the reusability of the Ca-based solid base catalyst while preserving its activity.

In this study, a calcium sodium silicate doped CaO was synthesized as a high-performance solid base catalyst for biodiesel production. The effect of calcination temperature on the catalyst composition, texture, and performance was investigated. Reaction parameters such as the reaction temperature, reaction time, methanol-to-oil ratio, and catalyst loading were studied to understand its catalytic behavior. The combined effect of the calcium sodium silicate and calcium oxide phase in NCSO on its performance was investigated. Catalyst reusability was evaluated in a series of continuous transesterification reactions for biodiesel production.

2. Results and Discussion

2.1. Catalyst Characterization

To understand the crystalline composition of the catalyst, XRD and SEM analyses were carried out on samples calcinated at different temperatures and the results are shown in Figure 1a–d (with standard PDF card) and Figure 2, respectively. When the sample was calcinated at 600 °C, only the Na_2CO_3 and NaNO_3 phases were shown, and no calcium species were found, indicating the existence of amorphous calcium species. During catalyst preparation, the concentration of CO_3^{2-} and SiO_3^{2-} were both 0.483 mol/L before the 1.45 mol/L Ca^{2+} -containing solution was added. Because the K_{sp} (solubility product constant) of CaCO_3 is 4.8×10^{-9} , which is lower than that of calcium silicates (for example, CaSiO_3 , 2.5×10^{-8}), CaCO_3 could be formed in favor of calcium silicates. Therefore, we deduced that the amorphous calcium species contains amorphous CaCO_3 and calcium silicate species. The SEM photo (Figure 2a) also prove that only irregular stacks of flake-like and granular solids were found. By increasing the calcination temperature to 800 °C, the $\text{Na}_2\text{CaSiO}_4$ phase emerged, a few Na_2CO_3 could still be found, and no other calcium silicates could be found. It could be deduced that the $\text{Na}_2\text{CaSiO}_4$ phase was formed by the solid-state reaction between calcium silicates or CaO (by decomposition of CaCO_3 at 600–700 °C) and sodium oxides, which was formed by the partial decomposition of Na_2CO_3 . By comparing the SEM photo (Figure 2b), we also noted that some ordered layered structures started to form when the calcination temperature increased. When the calcination temperature reached 950 °C, only $\text{Na}_2\text{CaSiO}_4$ could be found, and its peak was higher than it was at 800 °C, indicating the full decomposition of Na_2CO_3 . The SEM photo (Figure 2c,d) also revealed that the ordered layered crystal group found at 800 °C became a rectangular sheet stack with good crystallinity. Therefore, we concluded that the ordered layer crystal was the $\text{Na}_2\text{CaSiO}_4$ phase. This unique layered structure can increase the contact between the reactant and the active site of the catalyst during the transesterification process, which is beneficial to the transesterification reaction.

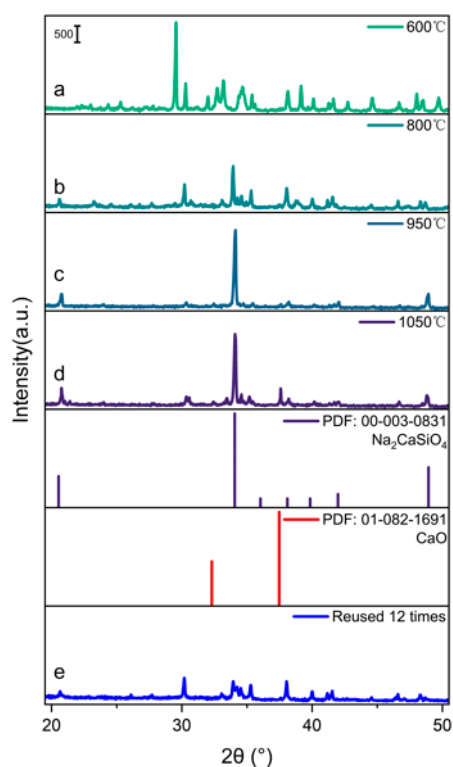


Figure 1. XRD spectrum of the NCSO catalyst calcinated at different temperatures (a–d) and the reused NCSO (e).

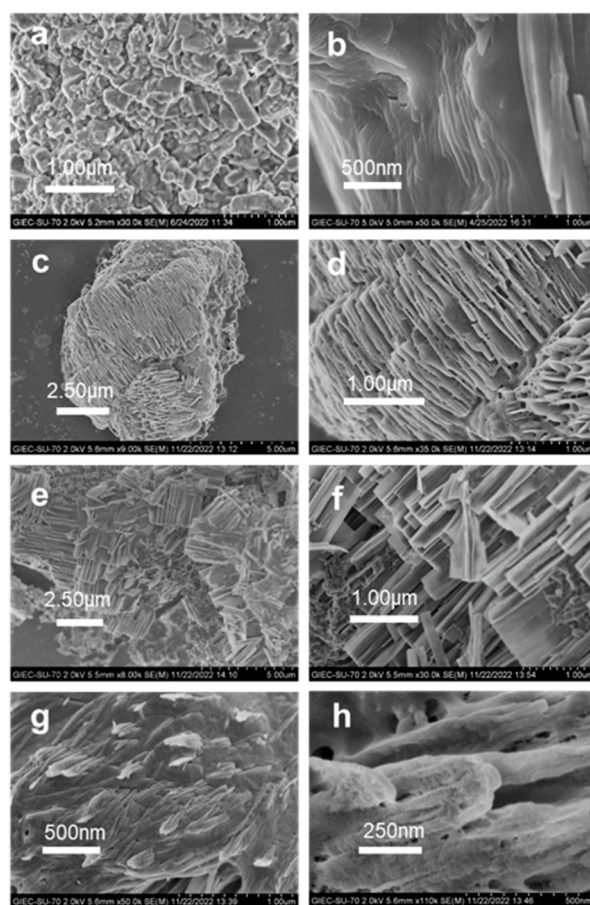


Figure 2. SEM images of the NCSO calcinated at different temperatures: (a) 600 °C; (b) 800 °C; (c,d) 950 °C; (e,f) 1050 °C; (g,h) NCSO reused for 12 cycles.

By further increasing the calcination temperature to 1050 °C, the CaO species emerged, and the peak $\text{Na}_2\text{CaSiO}_4$ was weaker than that at 950 °C. We also found that the sheets became thinner and sharper (Figure 2e,f) compared to that at 950 °C. Figure 1e presents the XRD result of the recycled catalyst, which was used for 12 batches of transesterification. The spectrum indicates the loss of the $\text{Na}_2\text{CaSiO}_4$ phase, consistent with its SEM photo: the edges of $\text{Na}_2\text{CaSiO}_4$ became blurred (Figure 2g,h), and the CaO species could also not be found.

Therefore, the main catalytic phase of this catalyst, which was named NCSO as follows, were $\text{Na}_2\text{CaSiO}_4$ and CaO.

2.2. Influence of Reaction Conditions on Biodiesel Production

To evaluate the effect of different reaction parameters on the NCSO-catalyzed conversion of soybean oil to biodiesel, different parameters including the reaction time, methanol/oil molar ratio, reaction temperature, and catalyst loading were studied. For experimental accuracy, all experiments were performed three times.

2.2.1. Influence of the Reaction Time

To investigate the effect of reaction time on the transesterification reaction of soybean oil and methanol, a series of reactions were carried out at a temperature of 80 °C, a molar ratio of methanol to oil of 9:1, and a catalyst content of 5 wt.%. The results are shown in Figure 3a. The transesterification reaction reached equilibrium at about 60 min with a biodiesel yield of 97.1%. Because the transesterification is reversible and trace water in the reaction media might cause the FAME saponification reaction in the base environment,

further lengthening the reaction time could lead a fluctuation in the FAME yield [25]. Therefore, we chose 60 min as the reaction time in a typical transesterification reaction.

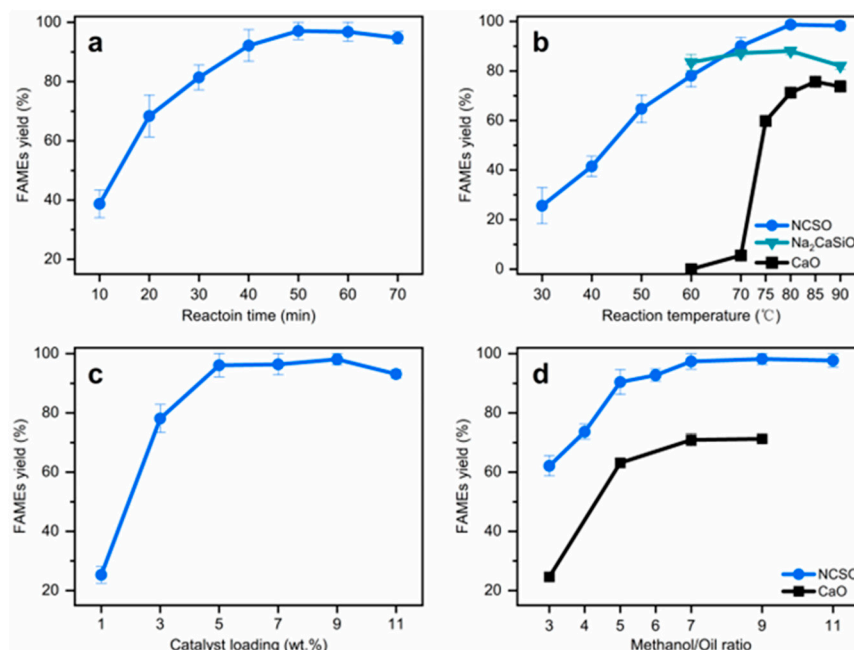


Figure 3. Effect of different reaction parameters on the transesterification reaction using NCSO: (a) reaction time; (b) reaction temperature; (c) catalyst loading; (d) methanol/oil molar ratio.

2.2.2. Influence of Reaction Temperature

The effect temperature on the transesterification reaction was studied at 30–90 °C, with 5 wt.% catalyst loading, and a 9:1 methanol/oil molar ratio, and the results are shown in Figure 3b. Due to the endothermic nature of this reaction, the FAME yield increased along with the temperature from 30 °C to 80 °C [29,30]. Additionally, increasing the temperature increased the molecular motion, leading to a greater chance to interact with the active site. On the other hand, an increase in temperature resulted in more dissolution of glycerol [31]. The biodiesel yield increased slowly when the temperature reached 60 °C or higher, and reached the maximum at 97.9% when the temperature was around 80 °C, indicating that the mass transfer resistance at the catalytic interface had largely been curbed.

To investigate the combined effect of Na₂CaSiO₄ and CaO in NCSO, Na₂CaSiO₄ was synthesized using the sol–gel method [32] (method and relative characterization mentioned in the Supplementary Materials, Figure S1. SEM, Figure S2. XRD) and used as a comparing catalyst for biodiesel production; the results are shown in Figure 3b. Under the same reaction conditions (catalyst loading 5 wt.%, methanol/oil ratio = 9:1), CaO (calcinated at 1050 °C) showed the lowest FAME yield. Especially at about 70–90 °C, both CaO and Na₂CaSiO₄ showed a lower FAME yield than NCSO. Therefore, we can conclude that there is a synergistic effect of CaO and FAMES in catalyzing transesterification reactions.

2.2.3. Influence of Catalyst Loading

To explore the effect of the amount of catalyst on the transesterification reaction of soybean oil and methanol, a series of reactions was carried out by changing the amount of catalyst (1–11%) at a methanol/oil ratio of 9:1 and reaction temperature of 80 °C; the results are shown in Figure 3c. The biodiesel yield increased correspondingly from 1% to 5% catalyst loading, reaching 97.5% at a 5 wt.% catalyst loading, which may be attributed to the increased contact opportunities between the catalyst and reactant at higher catalyst concentrations [33–35]. However, if the catalyst biodiesel continued to increase beyond 5%, there was no significant increase, and if the catalyst increased beyond 9%, the biodiesel yield began to decline. It may be that the rise in the amount of catalyst may make the reactant

mixture more viscous, and too much catalyst will lead to agglomeration [36], increasing the mass transfer resistance between the methanol–oil catalyst phase, resulting in difficulty in mixing the catalyst, reactants, and products, resulting in a lower oil conversion rate [37,38].

2.2.4. Influence of the Methanol/Oil Molar Ratio

According to a previous study on transesterification research, methanol activation on the solid base catalytic interface is the speed-limiting step in the transesterification reaction to produce biodiesel [39]. The effect of the methanol to oil molar ratio on the yield of FAMES was also studied using a 5 wt.% catalyst at a reaction temperature of 80 °C in the range of 3:1 to 11:1 for 60 min; the results are shown in Figure 3d. The stoichiometric ratio of the reactant in the biodiesel transesterification reaction as methanol/oil = 3:1. Under this situation, the NCSO catalyst could even show a 62.1% FAME yield, but only a 24.6% FAME yield when using CaO. This could be explained by the layered sheet structure in NCSO being able to effectively activate methanol, even under low methanol concentrations. The FAME yield remained stable from 7:1 to 9:1, ranging from 94.8% to 98.2%. These results indicate that the diluting effect of extra methanol did not impact the catalytic efficiency of NCSO under the given reaction conditions.

2.3. Reusability of NCSO

As Figure 4 shows, after being reused six times, NCSO retained about 95% of its maximum activity. Compared to the pure $\text{Na}_2\text{CaSiO}_4$, only 12.9% FAME yield remained after five times of reuse. As shown in Figure 1d,e (XRD) and Figure 2g,h (SEM), the compositions of NCSO changed, especially the reduced crystalline structure of the $\text{Na}_2\text{CaSiO}_4$ and CaO, which was also confirmed by the blurring edge of the layered-sheet structure in the fresh catalyst (Figure 2e,f). To explain the stability of NCSO and its catalytic behavior in consecutive batches of reaction, several characterizations were conducted.

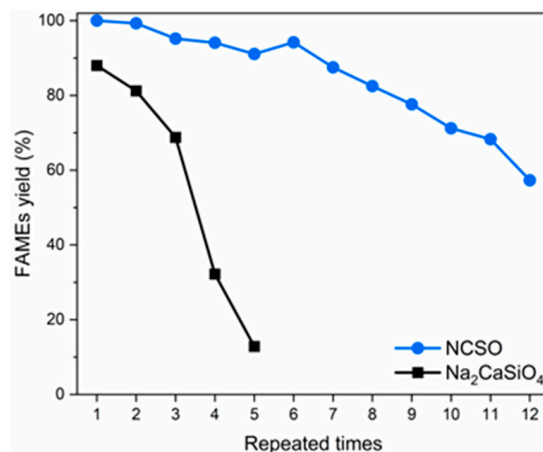


Figure 4. Reusability of the NCSO catalyst. Reaction conditions: molar ratio of methanol to oil = 9:1, agitation speed = 400 rpm, 9 wt.% catalyst loading, 80 °C, 60 min.

The XPS spectra of the fresh and recycled NCSO and pure $\text{Na}_2\text{CaSiO}_4$ were compared in Figure 5. According to previous reports, the binding energy (BE) of $\text{Ca}2p_{3/2}$ is 346.1 eV for pure CaO and 347.2 eV for CaCO_3 , compared to 346.4 eV, 347.1 eV, and 346.4 eV for the fresh NCSO, recycled NCSO, and $\text{Na}_2\text{CaSiO}_4$, respectively (Figure 5a–c). It was proven that the active Ca species in fresh NCSO showed quite similar activity to $\text{Na}_2\text{CaSiO}_4$ and became less active after being reused several times (the recycled NCSO showed a similar $\text{Ca}2p_{3/2}$ BE to CaCO_3 , which had been proven to be inactive for transesterification). In the crystal structure of $\text{Na}_2\text{CaSiO}_4$ (Figure S3), the Si species interact with the nearby O to form a tetrahedron $[\text{SiO}_4]$, which, especially in $\text{Na}_2\text{CaSiO}_4$, does not bridge other $[\text{SiO}_4]$ in the crystal. These oxygens in $[\text{SiO}_4]$ turn to interact with its nearby Na and Ca cations. With CaO in NCSO, the Si species in NCSO (Figure 5d) showed a much higher binding

energy ($\text{Si}2p_{3/2}$, 102.0 eV) than that in $\text{Na}_2\text{CaSiO}_4$ (Figure 5f, 100.8 eV), indicating a strong interaction between the CaO and the Si species from $\text{Na}_2\text{CaSiO}_4$ in NCSO [33]. The Si species in the recycled NCSO showed a much stronger binding energy (Figure 5e, 102.4 eV) than that in NCSO and $\text{Na}_2\text{CaSiO}_4$, indicating that some new silicates formed after being reused. O species in all researched samples showed O1s activity (Figure 5g–i), and O1s at 532.8 eV referred to the Si–O interaction as it remained stable after being reused. In contrast, O1s at 531.6–531.0 eV belonged to the metal–oxygen–silicon interaction. With CaO species in NCSO, the Ca–O–Si at the interface of CaO gave an O1s at 531.6 eV compared with 531.0 eV for Ca–O–Si or Na–O–Si, which dominated in the crystal phase of $\text{Na}_2\text{CaSiO}_4$. Thus, for the recycled group, O1s at 531.4 eV was in-between NCSO and $\text{Na}_2\text{CaSiO}_4$, indicating the loss of the CaO phase during batches of reaction. Figure 5j–l reflects the C species on all samples (except for the 284.8 eV C–C from contamination carbon). C1s at about 289.1 eV referred to the vertical linear absorption of CO_2 to cation M to form the M–O–C=O (M=Ca, Na) interaction, while the C1s at about 285.8 eV referred to the C–O species in the CaCO_3 [40,41].

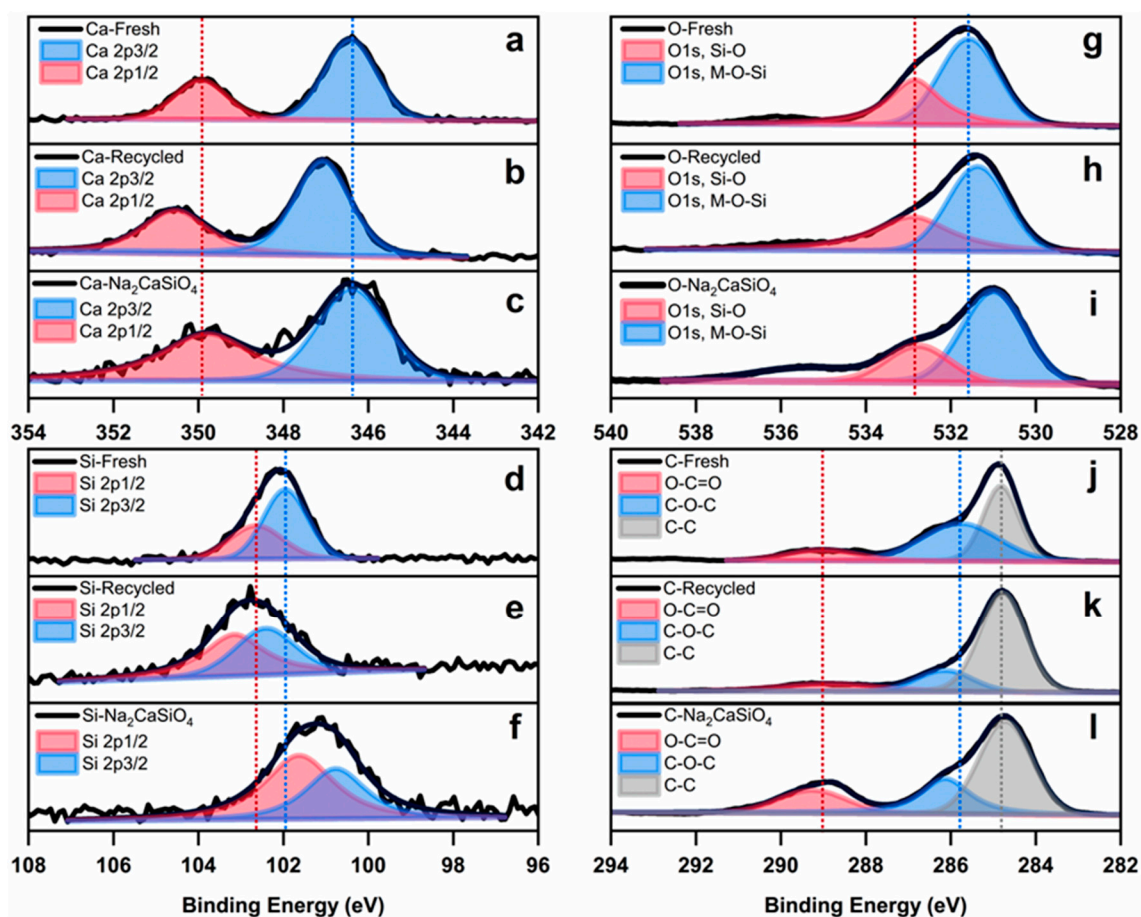


Figure 5. XPS analysis of the catalysts: (a,d,g,j) fresh NCSO; (b,e,h,k) recycled NCSO; (c,f,i,l) $\text{Na}_2\text{CaSiO}_4$.

The CO_2 absorbing behavior on the solid base mainly depends on the basicity of the catalyst sample. The results of the CO_2 -TPD analysis of NCSO and $\text{Na}_2\text{CaSiO}_4$ are shown in Figure 6.

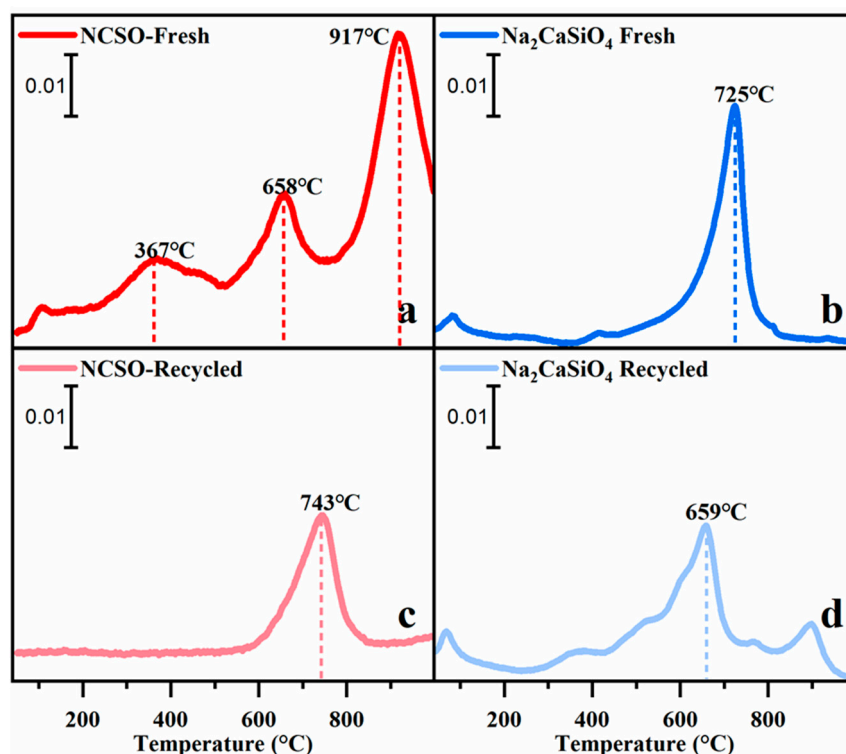


Figure 6. CO₂-TPD of NCSO and Na₂CaSiO₄: (a) fresh NCSO; (b) recycled NCSO (12 cycles); (c) fresh Na₂CaSiO₄; (d) recycled Na₂CaSiO₄ (5 cycles).

Fresh NCSO had two strong CO₂ desorption peaks at 658 °C and 917 °C, respectively, compared to only one at 725 °C for the Na₂CaSiO₄, and the total basicity was 2.22 mmol/g and 0.43 mmol/g, respectively. According to previous reports, CaO usually has a CO₂ desorption peak at 570–660 °C [42,43]. Therefore, we could confirm that the interaction between the CaO and Na₂CaSiO₄ phase provided stronger basic sites for NCSO than individually. The recycled samples showed an obvious loss of basic sites with the remaining total basic sites of 1.02 mmol/g and 0.23 mmol/g for NCSO (after 12 cycles, 57.3% FAME yield remaining) and Na₂CaSiO₄ (after five cycles, 12.9% FAME yield remaining), respectively, which also had weaker basicity than the fresh catalysts. This could indicate that the interaction between the [SiO₄] and CaO phase in NCSO, as confirmed in the XPS analysis, could help improve the stability of NCSO.

Although NCSO showed high activity and good reusability, the reason for its activity reduction should be discussed. First, regarding the leaching of CaO from NCSO, we noted that the recycled NCSO showed a similar basicity to the fresh Na₂CaSiO₄ (Figure 6b,c), proving that the CaO phase in NCSO could help to improve the basicity, and the loss of the CaO phase of NCSO was a reason for the reduced activity. XPS analysis on O1s revealed a Si–O–Ca BE shift, which could also prove the leaching of Ca species from NCSO. Second, mechanical stirring could make the catalyst leaching more serious. Therefore, more research is needed to strengthen the Ca–O species over Na₂CaSiO₄. Third, the destruction of the layered-sheet structure of NCSO during batches of reactions, as shown in Figure 2, led to a reduction in the activation efficiency of methanol, which was also a cause of the reduction in activity.

3. Materials and Methods

3.1. Materials

SiO₂ (600–800 mesh), CaO, and n-hexane were purchased from Shanghai Maclean Biochemical Technology Co. Na₂CO₃, NaOH, Ca(NO₃)₂·4H₂O, and methanol were purchased from Tianjin Fuchen Chemical Reagent Co. (Tianjin China), Tianjin Damao Chemical Reagent Factory (Tianjin China), and Tianjin Fuyu Fine Chemical Co. (Tianjin China). All

of the chemicals used were of analytical grade and hence used without further purification. Refined soybean oil used for transesterification by Yihai Kerry Company (shanghai, China) was obtained from the local supermarket in Guangzhou, China.

3.2. Catalyst Preparation

As shown in Figure 7, a 0.145 mol SiO_2 powder was added to a 100 mL aqueous solution containing 0.725 mole of NaOH under vigorous stirring at 80 °C. After the SiO_2 powder was completely reacted with NaOH, 100 mL of an aqueous solution containing 0.145 mol of Na_2CO_3 was added. Then, a 100 mL aqueous solution containing 0.145 mol of $\text{Ca}(\text{NO}_3)_2 \cdot 4\text{H}_2\text{O}$ was slowly added to the above-mixed solution. The formed slurry-like product was dried at 80 °C overnight. Finally, the dried solid powder was thoroughly ground, placed in a 100 mL crucible, heated in a muffle furnace at 5 °C/min to 1050 °C, and kept for 2 h. After cooling to room temperature, the catalyst was ground to powder and kept in a vacuum drier before it was used for further research.

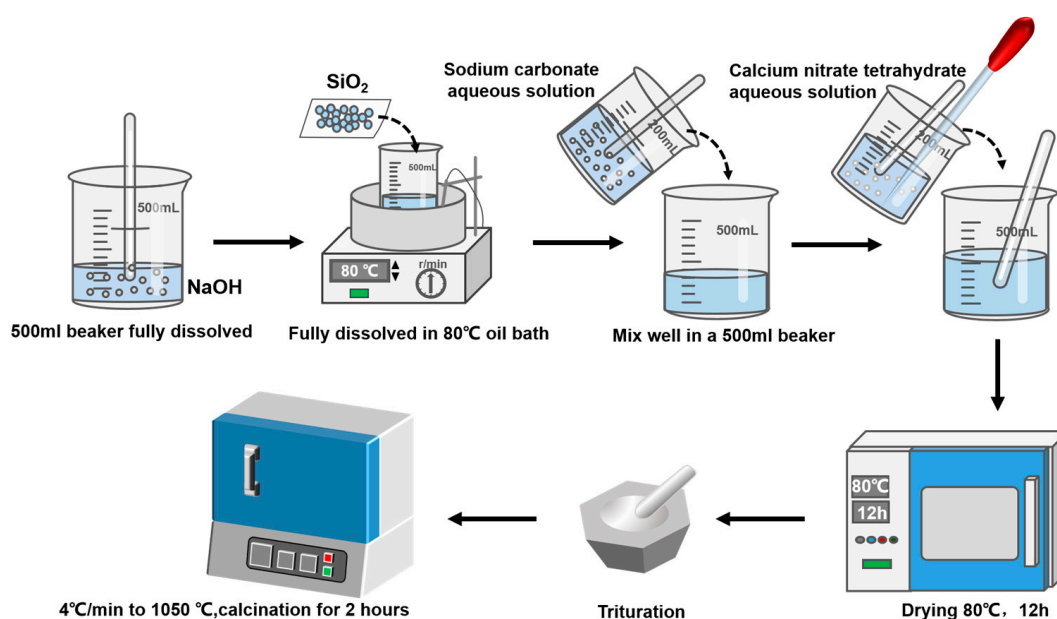


Figure 7. The NCSO catalyst preparation scheme.

3.3. Catalyst Characterization

The crystalline phases and the compositions of the catalysts were analyzed by X-ray diffraction (XRD, X'Pert Pro MPD, PANalytical, Almelo, The Netherlands) coupled with Cu $\text{K}\alpha$ radiation (40 kV and 40 mA). The diffraction data of the catalyst were recorded with 0.0167° steps over the 10~90° angular range.

X-ray photoelectron spectroscopy (XPS) measurements were performed on a Thermo Scientific ESCALAB 250 Xi X-ray photoelectron spectrometer (Waltham, MA, USA). The working voltage of the XPS was 20 kV, and the current was 10 mA. The C1s photoelectron peak (284.8 eV) was employed for the binding energy calibration.

The surface morphology of the sample was observed by scanning electron microscopy (SEM, S-4800 FESEM, HITACHI, Tokyo, Japan).

The elemental composition of the catalyst was analyzed by wavelength dispersive X-ray fluorescence spectrometry (XRF, AXIOSmAX-PETRO, PANalytical) measurements.

Temperature-programmed desorption of CO_2 (CO_2 -TPD, AutoChemII 2920, Micromeritics, Norcross, GA, USA) was conducted to determine the basicity and quantify the basic site of the samples. In a typical analysis, about 150 mg of solid catalyst is degassed in a helium flow. The sample is then saturated with CO_2 at ambient temperature. After being washed for 30 min with He flow, the catalyst is heated to 1000 °C at a heating rate of 10 °C/min.

3.4. Transesterification of Soybean Oil

The transesterification experiments were carried out in a 15 mL pressure-resistant flask, which was heated in an oil bath equipped with a magnetic stirrer. In a typical transesterification reaction, 0.6 g of methanol and 2.0 g of soybean oil were added into the reactor with 0.1 g of catalyst and a magnetic stirrer. Then, the reactor was put into the pre-heated oil bath at 80 °C with a stirring speed of 400 rpm; the reaction lasted 1 h. After the reaction, the mixture was cooled to room temperature in cold water and transferred into a 20 mL centrifuge tube. The biodiesel sample was separated using a centrifuge at 10,000 rpm for 5 min. The upper layer of liquid was washed with water to remove the methanol. The bottom layer of liquid, mainly glycerol, was also separated from the catalyst if the catalyst was meant to be recycled for further research. Finally, anhydrous calcium chloride was used to remove the residual water in the biodiesel sample before it was used in further analysis (biodiesel product and its GCMS spectral with molecular structure could be found in Figures S4 and S5 and Table S1 in the supplementary information, key properties of biodiesel product could be found in Table S2 in the supplementary information).

3.5. Product Analysis

The FAME content in the biodiesel products was quantified using GC (gas chromatography). A certain amount of the analyzed sample (ca. 20 mg) was added into a 5 mL volumetric flask and mixed with 1 mg of heptadecanoic acid methyl ester (dissolved in n-hexane) and the volume fixed with hexane to the scale line. The solution was filtered through a 0.25 µm needle filter and analyzed using a GC-2010 Plus (Shimadzu, Kyoto, Japan) with a flame ionization detector (FID) equipped with a capillary column (DB-WAX, 30 m × 0.25 mm × 0.25 µm). The chromatographic parameters were set as follows: the detector and injector temperatures were 300 °C and 250 °C, respectively; the column temperature started from 100 °C, rising at a rate of 20 °C/min until 185 °C and then 20 °C/min until 225 °C, before finally being increased to 240 °C at 20 °C/min and held for 3 min. Argon was used as a carrier gas with a flow rate of 40 cm/s. The yield of biodiesel is defined as:

$$\text{Biodiesel yield} = \frac{V \times \sum c_i}{m}$$

where m , c_i , and V are the mass of the product to be measured, the concentration of each fatty acid methyl ester, and the constant volume of the volumetric flask, respectively.

4. Conclusions

In this paper, a silicate-strength strategy was adopted to synthesize a solid base catalyst NSCO. The catalyst precursor was calcinated at 1050 °C to give NCSO two main catalytic phases, $\text{Na}_2\text{CaSiO}_4$ and CaO. Those two phases showed a synergistic effect, enabling NCSO to have high activity and good reusability. The layered-like-sheet structure in NCSO allowed for a higher methanol activation efficiency at a low methanol concentration when compared to CaO. A 98.2% FAME yield could be achieved in 60 min at 80 °C with a 9:1 methanol/oil molar ratio and 5 wt.% catalyst loading. A 94.3% FAME yield could still be achieved even after six consecutive reuses. This silicate-strength strategy provides a new way to improve the stability while retaining the activity of the calcium-based base catalyst.

Supplementary Materials: The following supporting information can be downloaded at: <https://www.mdpi.com/article/10.3390/catal13040775/s1>, Figure S1: SEM picture of the as-synthesized $\text{Na}_2\text{CaSiO}_4$; Figure S2: XRD result of the as-synthesized $\text{Na}_2\text{CaSiO}_4$; Figure S3: Crystal structure of $\text{Na}_2\text{CaSiO}_4$; Figure S4: GCMS spectra of biodiesel; Figure S5: Biodiesel product from soybean oil; Table S1: Molecular structures for biodiesel by GCMS; Table S2: Key properties of biodiesel product from soybean oil.

Author Contributions: Conceptualization, J.F.; Methodology, S.Z. and J.F.; Validation, J.F. and X.L.; Formal analysis, J.F. and S.Z.; Investigation, S.Z. and J.F.; Validation, S.Z. and J.F.; Resources, S.X. and J.F.; Data curation, S.Z. and J.F.; Writing—original draft, S.Z. and J.F.; Writing—review and editing, J.F. and M.L.; Supervision, L.Y. and P.L.; Funding acquisition, P.L. All authors have read and agreed to the published version of the manuscript.

Funding: This research was funded by the National Key Research and Development Project of China (2022YFE0207100); the Foundation of Key Laboratory of Renewable Energy, Chinese Academy of Sciences (2021000024); the National Natural Science Foundation of China (52206286, 32271822, 51903236); the Guangdong Basic and Applied Basic Research Foundation (2022A1515010440).

Data Availability Statement: Data are contained within the article and are available from the first corresponding author.

Conflicts of Interest: The authors declare no conflict of interest.

References

1. Zul, N.A.; Ganesan, S.; Hamidon, T.S.; Oh, W.-D.; Hussin, M.H. A review on the utilization of calcium oxide as a base catalyst in biodiesel production. *J. Environ. Chem. Eng.* **2021**, *9*, 105741. [[CrossRef](#)]
2. Munyentwali, A.; Li, H.; Yang, Q. Review of advances in bifunctional solid acid/base catalysts for sustainable biodiesel production. *Appl. Catal. A Gen.* **2022**, *633*, 118525. [[CrossRef](#)]
3. Orege, J.I.; Oderinde, O.; Kifle, G.A.; Ibikunle, A.A.; Raheem, S.A.; Ejeromedoghene, O.; Okeke, E.S.; Olukowi, O.M.; Orege, O.B.; Fagbohun, E.O.; et al. Recent advances in heterogeneous catalysis for green biodiesel production by transesterification. *Energy Convers. Manag.* **2022**, *258*, 115406. [[CrossRef](#)]
4. Jamil, U.; Husain Khoja, A.; Liaquat, R.; Raza Naqvi, S.; Nor Nadyaini Wan Omar, W.; Aishah Saidina Amin, N. Copper and calcium-based metal organic framework (MOF) catalyst for biodiesel production from waste cooking oil: A process optimization study. *Energy Convers. Manag.* **2020**, *215*, 112934. [[CrossRef](#)]
5. Demirbas, A. Biodiesel from waste cooking oil via base-catalytic and supercritical methanol transesterification. *Energy Convers. Manag.* **2009**, *50*, 923–927. [[CrossRef](#)]
6. Yildiz, I.; Acikkalp, E.; Caliskan, H.; Mori, K. Environmental pollution cost analyses of biodiesel and diesel fuels for a diesel engine. *J. Environ. Manag.* **2019**, *243*, 218–226. [[CrossRef](#)]
7. Qiu, F.; Li, Y.; Yang, D.; Li, X.; Sun, P. Biodiesel production from mixed soybean oil and rapeseed oil. *Appl. Energy* **2011**, *88*, 2050–2055. [[CrossRef](#)]
8. Liu, X.; Xing, S.; Yang, L.; Fu, J.; Lv, P.; Zhang, X.; Li, M.; Wang, Z. Highly active and durable Ca-based solid base catalyst for biodiesel production. *Fuel* **2021**, *302*, 121094. [[CrossRef](#)]
9. Lee, J.C.; Lee, B.; Ok, Y.S.; Lim, H. Preliminary techno-economic analysis of biodiesel production over solid-biochar. *Bioresour. Technol.* **2020**, *306*, 123086. [[CrossRef](#)]
10. Ma, Y.; Wang, Q.; Sun, X.; Wu, C.; Gao, Z. Kinetics studies of biodiesel production from waste cooking oil using FeCl₃-modified resin as heterogeneous catalyst. *Renew. Energy* **2017**, *107*, 522–530. [[CrossRef](#)]
11. Rabie, A.M.; Shaban, M.; Abukhadra, M.R.; Hosny, R.; Ahmed, S.A.; Negm, N.A. Diatomite supported by CaO/MgO nanocomposite as heterogeneous catalyst for biodiesel production from waste cooking oil. *J. Mol. Liq.* **2019**, *279*, 224–231. [[CrossRef](#)]
12. Chen, G.-Y.; Shan, R.; Yan, B.-B.; Shi, J.-F.; Li, S.-Y.; Liu, C.-Y. Remarkably enhancing the biodiesel yield from palm oil upon abalone shell-derived CaO catalysts treated by ethanol. *Fuel Process. Technol.* **2016**, *143*, 110–117. [[CrossRef](#)]
13. Kouzu, M.; Hidaka, J.-s. Transesterification of vegetable oil into biodiesel catalyzed by CaO: A review. *Fuel* **2012**, *93*, 1–12. [[CrossRef](#)]
14. Mazaheri, H.; Ong, H.C.; Amini, Z.; Masjuki, H.H.; Mofijur, M.; Su, C.H.; Anjum Badruddin, I.; Khan, T.M.Y. An Overview of Biodiesel Production via Calcium Oxide Based Catalysts: Current State and Perspective. *Energies* **2021**, *14*, 3950. [[CrossRef](#)]
15. Teo, S.H.; Rashid, U.; Choong, S.Y.T.; Taufiq-Yap, Y.H. Heterogeneous calcium-based bimetallic oxide catalyzed transesterification of *Elaeis guineensis* derived triglycerides for biodiesel production. *Energy Convers. Manag.* **2017**, *141*, 20–27. [[CrossRef](#)]
16. Sudsakorn, K.; Saiwuttikul, S.; Palitsakun, S.; Seubsai, A.; Limtrakul, J. Biodiesel production from *Jatropha Curcas* oil using strontium-doped CaO/MgO catalyst. *J. Environ. Chem. Eng.* **2017**, *5*, 2845–2852. [[CrossRef](#)]
17. Dias, A.P.S.; Ramos, M. On the storage stability of CaO biodiesel catalyst. Hydration and carbonation poisoning. *J. Environ. Chem. Eng.* **2021**, *9*, 104917. [[CrossRef](#)]
18. Malins, K. The potential of K₃PO₄, K₂CO₃, Na₃PO₄ and Na₂CO₃ as reusable alkaline catalysts for practical application in biodiesel production. *Fuel Process. Technol.* **2018**, *179*, 302–312. [[CrossRef](#)]
19. de Lima, A.L.; Ronconi, C.M.; Mota, C.J.A. Heterogeneous basic catalysts for biodiesel production. *Catal. Sci. Technol.* **2016**, *6*, 2877–2891. [[CrossRef](#)]
20. Rahmani Vahid, B.; Haghghi, M. Urea-nitrate combustion synthesis of MgO/MgAl₂O₄ nanocatalyst used in biodiesel production from sunflower oil: Influence of fuel ratio on catalytic properties and performance. *Energy Convers. Manag.* **2016**, *126*, 362–372. [[CrossRef](#)]

21. Rodríguez-Ramírez, R.; Romero-Ibarra, I.; Vazquez-Arenas, J. Synthesis of sodium zincsilicate ($\text{Na}_2\text{ZnSiO}_4$) and heterogeneous catalysis towards biodiesel production via Box-Behnken design. *Fuel* **2020**, *280*, 118668. [[CrossRef](#)]
22. Ibrahim, M.L.; Nik Abdul Khalil, N.N.A.; Islam, A.; Rashid, U.; Ibrahim, S.F.; Sinar Mashuri, S.I.; Taufiq-Yap, Y.H. Preparation of Na_2O supported CNTs nanocatalyst for efficient biodiesel production from waste-oil. *Energy Convers. Manag.* **2020**, *205*, 112445. [[CrossRef](#)]
23. Sánchez Faba, E.M.; Ferrero, G.O.; Dias, J.M.; Eimer, G.A. Na-Ce-modified-SBA-15 as an effective and reusable bimetallic mesoporous catalyst for the sustainable production of biodiesel. *Appl. Catal. A Gen.* **2020**, *604*, 117769. [[CrossRef](#)]
24. Rijo, B.; Fernando, E.; Ramos, M.; Dias, A.P.S. Biodiesel production over sodium carbonate and bicarbonate catalysts. *Fuel* **2022**, *323*, 124383. [[CrossRef](#)]
25. Wan, L.; Liu, H.; Skala, D. Biodiesel production from soybean oil in subcritical methanol using MnCO_3/ZnO as catalyst. *Appl. Catal. B Environ.* **2014**, *152–153*, 352–359. [[CrossRef](#)]
26. Wang, J.; Yang, L.; Luo, W.; Yang, G.; Miao, C.; Fu, J.; Xing, S.; Fan, P.; Lv, P.; Wang, Z. Sustainable biodiesel production via transesterification by using recyclable $\text{Ca}_2\text{MgSi}_2\text{O}_7$ catalyst. *Fuel* **2017**, *196*, 306–313. [[CrossRef](#)]
27. Wang, J.; Wang, Z.; Yang, L.; Yang, G.; Miao, C.; Lv, P. Natural albite as a novel solid basic catalyst for the effective synthesis of biodiesel: Characteristics and performance. *Energy* **2017**, *141*, 1650–1660. [[CrossRef](#)]
28. Pavlović, S.M.; Marinković, D.M.; Kostić, M.D.; Janković-Častvan, I.M.; Mojović, L.V.; Stanković, M.V.; Veljković, V.B. A CaO/zeolite-based catalyst obtained from waste chicken eggshell and coal fly ash for biodiesel production. *Fuel* **2020**, *267*, 117171. [[CrossRef](#)]
29. Singh, V.; Hameed, B.H.; Sharma, Y.C. Economically viable production of biodiesel from a rural feedstock from eastern India, *P. pinnata* oil using a recyclable laboratory synthesized heterogeneous catalyst. *Energy Convers. Manag.* **2016**, *122*, 52–62. [[CrossRef](#)]
30. Samart, C.; Sreetongkittikul, P.; Sookman, C. Heterogeneous catalysis of transesterification of soybean oil using KI/mesoporous silica. *Fuel Process. Technol.* **2009**, *90*, 922–925. [[CrossRef](#)]
31. Bahador, F.; Foroutan, R.; Nourafkan, E.; Peighambaroust, S.J.; Esmaeili, H. Enhancement of Biodiesel Production from Chicken Fat Using MgO and MgO@ Na_2O Nanocatalysts. *Chem. Eng. Technol.* **2020**, *44*, 77–84. [[CrossRef](#)]
32. Koppala, S.; Swamiappan, S. Glowing Combustion Synthesis, Characterization, and Toxicity Studies of $\text{Na}_2\text{CaSiO}_4$ Powders. *Mater. Manuf. Process.* **2015**, *30*, 1476–1481. [[CrossRef](#)]
33. Huang, J.; Zou, Y.; Yaseen, M.; Qu, H.; He, R.; Tong, Z. Fabrication of hollow cage-like CaO catalyst for the enhanced biodiesel production via transesterification of soybean oil and methanol. *Fuel* **2021**, *290*, 119799. [[CrossRef](#)]
34. Roschat, W.; Phewphong, S.; Thangthong, A.; Moonsin, P.; Yoosuk, B.; Kaewpuang, T.; Promarak, V. Catalytic performance enhancement of CaO by hydration-dehydration process for biodiesel production at room temperature. *Energy Convers. Manag.* **2018**, *165*, 1–7. [[CrossRef](#)]
35. Wang, J.-X.; Chen, K.-T.; Wu, J.-S.; Wang, P.-H.; Huang, S.-T.; Chen, C.-C. Production of biodiesel through transesterification of soybean oil using lithium orthosilicate solid catalyst. *Fuel Process. Technol.* **2012**, *104*, 167–173. [[CrossRef](#)]
36. Yan, B.; Zhang, Y.; Chen, G.; Shan, R.; Ma, W.; Liu, C. The utilization of hydroxyapatite-supported CaO-CeO₂ catalyst for biodiesel production. *Energy Convers. Manag.* **2016**, *130*, 156–164. [[CrossRef](#)]
37. Chen, G.-Y.; Shan, R.; Shi, J.-F.; Yan, B.-B. Transesterification of palm oil to biodiesel using rice husk ash-based catalysts. *Fuel Process. Technol.* **2015**, *133*, 8–13. [[CrossRef](#)]
38. Shan, R.; Zhao, C.; Yuan, H.; Wang, S.; Wang, Y. Transesterification of vegetable oil using stable natural diatomite-supported catalyst. *Energy Convers. Manag.* **2017**, *138*, 547–555. [[CrossRef](#)]
39. Tasić, M.B.; Stamenković, O.S.; Veljković, V.B. Cost analysis of simulated base-catalyzed biodiesel production processes. *Energy Convers. Manag.* **2014**, *84*, 405–413. [[CrossRef](#)]
40. Albuquerque, M.C.G.; Azevedo, D.C.S.; Cavalcante, C.L.; Santamaría-González, J.; Mérida-Robles, J.M.; Moreno-Tost, R.; Rodríguez-Castellón, E.; Jiménez-López, A.; Maireles-Torres, P. Transesterification of ethyl butyrate with methanol using MgO/CaO catalysts. *J. Mol. Catal. A Chem.* **2009**, *300*, 19–24. [[CrossRef](#)]
41. Black, L.; Garbev, K.; Stemmermann, P.; Hallam, K.R.; Allen, G.C. Characterisation of crystalline C-S-H phases by X-ray photoelectron spectroscopy. *Cem. Concr. Res.* **2003**, *33*, 899–911. [[CrossRef](#)]
42. Shan, R.; Chen, G.; Yan, B.; Shi, J.; Liu, C. Porous CaO-based catalyst derived from PSS-induced mineralization for biodiesel production enhancement. *Energy Convers. Manag.* **2015**, *106*, 405–413. [[CrossRef](#)]
43. Tang, Y.; Liu, H.; Ren, H.; Cheng, Q.; Cui, Y.; Zhang, J. Development KCl/CaO as a catalyst for biodiesel production by tri-component coupling transesterification. *Environ. Prog. Sustain. Energy* **2018**, *38*, 647–653. [[CrossRef](#)]

Disclaimer/Publisher's Note: The statements, opinions and data contained in all publications are solely those of the individual author(s) and contributor(s) and not of MDPI and/or the editor(s). MDPI and/or the editor(s) disclaim responsibility for any injury to people or property resulting from any ideas, methods, instructions or products referred to in the content.